Near-field ground motion during earthquake preparation process

M D SHARMA

Department of Atmospheric and Oceanic Sciences, Kurukshetra University, Kurukshetra 136 119, India

Wave number discretization method is applied to study the near-field of seismic sources embedded in a cracked elastic solid. Near-field solutions are obtained for horizontal and vertical line forces. Effects of modifications in cracks of focal region on ground motion, in the near-field, are studied numerically for different

- values of crack density,
- saturation of cracks,
- width of cracks, and
- regimes of connection between cracks.

An earthquake process is assumed to be going through five major stages. These stages represent continuous accumulation of stress, interconnections between cracks leading to eventual failure and drainage of fluid from cracks after the major shock. Variations in the velocity ratio of waves noted from accelerograms verify the process of preparation of an earthquake. P wave contribution to vertical acceleration is negligible when the source is a vertical line force and S wave contributes only a little to horizontal acceleration when the source is a horizontal line force.

1. Introduction

Recent studies suggest that there is a distribution of liquid-filled cracks throughout at least the top 10–20 km of the crust. The effects of cracks on seismic waves are important since seismic experiments are one of the few geophysical techniques capable of examining the properties of rocks in the crust. It has applications to many currently important activities ranging from determining the preferred direction of flow in hydrocarbon reservoirs to earthquake prediction.

Nur (1972) and Aggarwal *et al* (1973) explained the travel time variations prior to an earthquake in terms of the changes in dilatancy around the focal zone and saturation of dilatancy-formed cracks. The wave velocities for the cracked elastic solids have been approximated by Garvin and Knopoff (1973, 1975a,b). O'Connell and Budiansky (1974) and Budiansky and O'Connell (1976) calculated the effects of the introduction of cracks on the elastic properties of an isotropic solid using self-consistent procedure. O'Connell and Budiansky (1977) studied the viscoelastic properties of cracked solid and explained three separate regimes of connection between cracks. Attenuation of elastic waves in the cracked solids have been studied by Chatterjee *et al* (1980), Hudson (1981) and Xu and King (1990). Hudson (1990a) and Peacock and Hudson (1990) studied the elastic properties of materials for different distribution of small cracks. Hudson (1990b) discussed the attenuation due to scattering in cracked materials.

Crampin (1985) suggested that the distribution of aligned water-filled cracks are widespread in the upper crust. Crampin (1987) explained that the most direct effect of the change of stress before an earthquake are the modifications in the cracks present in and around the focal region. These modifications are the common driving mechanism for a large variety of precursors observed before earthquakes.

Keywords. Wave number discretization; crack density; saturation; aspect ratio; synthetic seismogram; line force.

Proc. Indian Acad. Sci. (Earth Planet. Sci.), **106**, Nos 1 & 2, June 1997, pp. 15–26

Particle displacement may be suggested as a way of monitoring the build-up of stress before earthquakes. The ability to estimate crack parameters and stress generation by analysing the near-field strong ground motion has widespread applications. Therefore, it is considered essential to observe and interpret the effects of stress changes on strong ground motion in a vulnerable area.

In this paper I propose to study ground motion in the near-field of seismic sources. Near-field represents the distance of few kilometers from an expected epicentre. An earthquake preparation region is assumed to be an elastic medium pervaded by a random distribution of water-filled cracks. In such a region, just before an earthquake, the increase or accumulation of local stresses are assumed enough to connect the cracks and permitting flow of liquid there. During the earthquake preparation process the changes in ground motion observed at the surface of the earth above this region, may be used as a precursor for an impending earthquake. The strong ground motion is calculated by a numerical technique presented by Bouchon and Aki (1977). This technique is applicable, specially, to study the near-field of a seismic source.

2. Cracked elastic solid

Studies discussed in the previous section explain the modifications in elastic moduli and changes in wave velocities when small cracks are introduced in an elastic solid. Most of these studies assume very small value of crack density but O'Connell and Budiansky (1974) assume no restriction on the value of crack density but consider only random distribution of cracks. O'Connell and Budiansky (1977) allow consideration of interconnections between cracks.

In fact, the cracks in the earth are accepted to be vertically aligned and strictly isolated (Crampin 1985, 1987). A medium with such a distribution of cracks behaves anisotropic to wave propagation. According to Crampin and Atkinson (1985), before an earthquake occurs, the local stresses may be large enough to promote crack growth sufficient to connect the micro cracks and permit water to flow into the region of greater dilatancy near the eventual fracture. Therefore, to consider the large values of crack density as well as interconnections between cracks, I preferred the effective elastic moduli derived by O'Connell and Budiansky (1974). They suggested that the effects of cracks of any convex shape would be similar to those of circular cracks provided the crack density ϵ is expressed in terms of area and perimeter of the cracks. Therefore the results for circular cracks may be used for more general cases with negligible error.

Consider an elastic solid containing a random distribution of circular cracks of radius a and thickness c, with very small aspect ratio c/a. Cracks are saturated by a fluid of bulk modulus $\tilde{K}$. Elastic constants are modified according to the regimes of connection between the cracks, defined by O'Connell and Budiansky (1977). Modified elastic constants in different interconnection regimes are explained as follows:

- *Saturated isolated*: No fluid is able to flow out of (or into) any crack. Changes in fluid pressure due to the application of external stress will be different in every crack. It represents a situation which arises for elastic waves of sufficiently high frequency. In such a situation the moduli found are appropriate for stress changes that occur sufficiently rapidly to prevent communication of fluid pressure between the cracks. Following Budiansky and O'Connell (1976), the elastic constants of the cracked solids are given by

$$\bar{K}/K = 1 - (16/9)\{(1 - \bar{\nu}^2)/(1 - 2\bar{\nu})\}D\epsilon, \tag{1}$$

$$\bar{\mu}/\mu = 1 - (32/45)(1 - \bar{\nu})\{D + 3/(2 - \bar{\nu})\}\epsilon, \tag{2}$$

where $K(= \lambda + 2\mu/3)$ is bulk modulus with λ and μ as Lame's constants. Poisson's ratio, ν, of the uncracked solid is $0.5\lambda/(\lambda + \mu)$. The barred quantities represent corresponding elastic parameters for saturated cracked solid. Following Sharma (1996), the saturation parameter D is expressed in terms of elastic constants and crack density as

$$\begin{aligned}\epsilon D(1 - \bar{\nu}^2) = {} & 45(\nu - \bar{\nu})/\{16(1 + 3\nu)\} \\ & + 2\epsilon(1 - 2\nu)(1 - \bar{\nu}^2)/ \\ & \{(1 + 3\nu)(2 - \bar{\nu})\}.\end{aligned} \tag{3}$$

Effective Poisson's ratio ($\bar{\nu}$) is computed numerically from a fifth degree equation for given values of ϵ, ν and another saturation parameter Ω, defined by

$$\Omega = \frac{a}{c}\frac{\tilde{K}}{K}. \tag{4}$$

For circular cracks (radius $= a$), volume of a sample crack (thickness $= c$) is given by $\frac{4}{3}\pi a^2 c$. Crack porosity (β_c) measures the fraction of volume occupied by cracks and is related to crack density (ϵ) by

$$\beta_c = \frac{4}{3}\pi\frac{c}{a}\epsilon. \tag{5}$$

The density of cracked solid ($\bar{\rho}$) is modified as

$$\bar{\rho} = (1 - \beta_c)\rho_s + \beta_c\rho_f, \tag{6}$$

where ρ_s denotes the density of solid in the absence of cracks and ρ_f is the density of the fluid present in the cracks. Partial saturation of cracks is represented by a parameter ξ. The ξ denotes the fraction of cracks which are fully saturated, in the unit volume

of bulk material. Elastic constants for partially saturated cracked solid are obtained by replacing D with $1-\xi+D\xi$. Density of such a solid is given by

$$\bar{\rho} = (1-\beta_c)\rho_s + \xi\beta_c\rho_f. \tag{7}$$

■ *Saturated isobaric*: All the cracks are in communication with each other but no fluid flow is permitted out of the bulk sample. Fluid pressure will be the same in all the cracks. Effective Poisson's ratio ($\bar{\nu}$) is obtained from

$$\epsilon = (45/16)(\nu-\bar{\nu})(2-\bar{\nu})/\{(1-\bar{\nu}^2)(10\nu-\bar{\nu}-3\nu\bar{\nu})\}, \tag{8}$$

for given values of ν and ϵ. Effective elastic moduli are derived from the relations, given by

$$\bar{K}/K = 1, \tag{9}$$

$$\bar{\mu}/\mu = 1-\{(32/45)(1-\bar{\nu})(5-\bar{\nu})/(2-\bar{\nu})\}\epsilon. \tag{10}$$

Density of the bulk material is given by (6).

■ *Drained*: The fluid in cracks is in communication with the outside of the sample. The saturated cracked solid will respond as if there was no fluid there. The elastic behavior will be equivalent to the cracked solid with dry cracks. The effective Poisson's ratio ($\bar{\nu}$) is obtained from equation (8). Using this value of $\bar{\nu}$, effective elastic moduli are obtained from (1)--(2) by substituting $D=1$. Density is given by (6).

3. Wave number discretization method

The steady state radiations from a line source in an infinite homogeneous medium can be represented as a continuous superposition of homogeneous and inhomogeneous plane waves. A technique assumes a periodic description of source and considers an infinite number of such sources distributed in a straight line at equal intervals. The distance between these sources is assumed enough so that perturbations from the neighbouring sources could reach the recording station only after the time interval of interest. This technique, presented by Bouchon and Aki (1977), enables to calculate the ground motion even in the regions which are very near to the focus. Following Bouchon and Aki (1977), the displacements or stresses in (x,z) plane, with source axis along y-direction, can be written in the form

$$F(x,z;\omega) = \int_{-\infty}^{\infty} f(k,z)e^{-ikx}\,\mathrm{d}k, \tag{11}$$

where k is horizontal wave number and ω is circular frequency. Time dependence is given by $e^{i\omega t}$.

Considering an infinite number of such sources distributed along the x-axis, at equal interval L, the total radiation takes the form

$$G(x,z;\omega) = \int_{-\infty}^{\infty} f(k,z)e^{-ikx}\sum_{m=-\infty}^{\infty} e^{ikml}\,\mathrm{d}k. \tag{12}$$

Following Bouchon and Aki (1977), results of distribution theory are used to write equation (12) as

$$G(x,z;\omega) = \frac{2\pi}{L}\sum_{n=-\infty}^{\infty} f(k_n,z)\exp(-ik_nx) \tag{13}$$

with discrete wave number $k_n = \frac{2\pi}{L}n$. If the infinite series converges then for each frequency there must exist some integer N such that infinite series can be approximated to finite sum equation, given by

$$G(x,z;\omega) = \frac{2\pi}{L}\sum_{n=-N}^{N} f(k_n,z)\exp(-ik_nx). \tag{14}$$

4. Definition of the problem

Assumed model considers a semi-infinite half-space consisting of an elastic solid containing a random distribution of liquid-filled cracks. Rectangular Cartesian coordinate system (x,y,z) is chosen with z-axis pointing vertically downwards into the medium. Plane $z=0$ represents the stress free surface, as shown in figure 1. The source is buried at $(x_0,0,z_0)$. The problem considers two-dimensional motion in

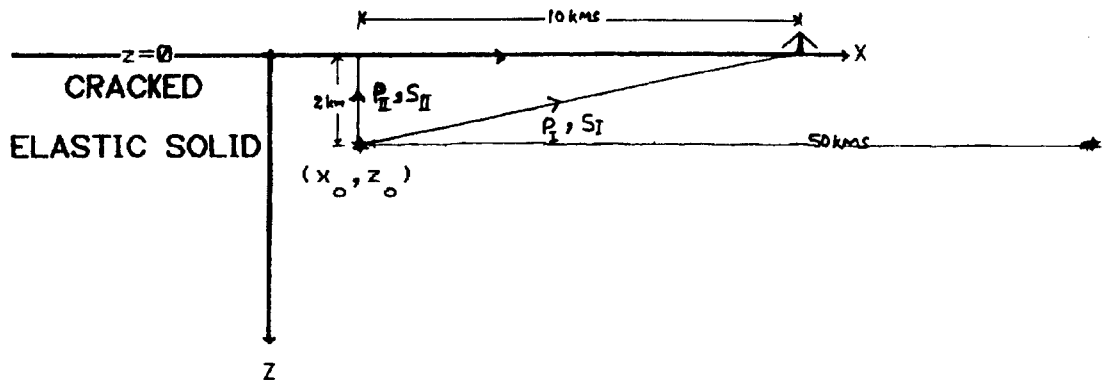

Figure 1. Geometry of the problem considered.

(x, z) plane and components along y-direction vanish. Displacement components $(u_x, 0, u_z)$ are defined as

$$u_x = \partial\phi/\partial x + \partial\psi/\partial z$$
$$u_z = \partial\phi/\partial z - \partial\psi/\partial x, \quad (15)$$

where ϕ and ψ represent potentials for compressional and shear wave respectively.

Solutions are obtained for general sources consisting of vertical line force or horizontal line force. Solutions for realistic sources such as seismic dislocations can be constructed by linear operations on single horizontal and vertical force solutions (Burridge and Knopoff 1964).

Earthquake preparation process is represented by the continuous increase of stress around the focal region of eventual failure. It is expected that increase or accumulation of stress in a rockmass

- Initiates crack growth and hence increases crack density ϵ.
- Decreases saturation degree ξ of cracks by crack growth or opening of new cracks at high stress.
- Increases the aspect ratio c/a of cracks due to growth of cracks. The change in aspect ratio is considered to be the most likely change of crack geometry in an earthquake preparation zone.
- Connects the microcracks and permits water to flow into dilatant region, when the stresses are great enough. Changes experienced by the interstitial liquid are taken into account while discussing the regimes of connection between cracks.

So, to study the effects of accumulation of stress on ground motion, it is required to observe and interpret strong ground motion with the variations in ϵ, c/a, ξ and crack interconnections leading to eventual failure.

5. Near-field ground motion

It is required to record perturbations due to a particular source, say at (x_0, z_0), alone for a time interval sufficient to analyse the ground motion. This requires the recording station to be near to this source. However, the distance between the source and recording station can be changed but this will require making a change in distance between the sources so that disturbance from the neighbouring sources reach only after the time interval of interest. Following Bouchon and Aki (1977) displacement potentials due to an internal vertical line force $Q_v e^{i\omega t}$, applied at (x_0, z_0) in the positive z-direction are

$$\phi_v = sgn(z - z_0)\frac{Q_v}{2L\mu k_\beta^2} \times \sum_{n=-N}^{N} \exp\{-\nu_n|z - z_0| - ik_n(x - x_0)\},$$

$$\psi_v = -\frac{Q_v}{2L\mu k_\beta^2}\sum_{n=-N}^{N}(ik_n/\gamma_n) \times \exp\{-\gamma_n|z - z_0| - ik_n(x - x_0)\}, \quad (16)$$

where

$$\nu_n = \sqrt{k_n^2 - k_\alpha^2}, \quad \mathrm{Re}(\nu_n) > 0; \quad k_\alpha = \omega/\alpha \quad (17)$$

and

$$\gamma_n = \sqrt{k_n^2 - k_\beta^2}, \quad \mathrm{Re}(\gamma_n) > 0; \quad k_\beta = \omega/\beta. \quad (18)$$

α and β denote the velocities of compressional and shear waves respectively.

Solving the stress free boundary conditions at the surface $z = 0$ yields the potentials to calculate surface displacements. Following Sharma and Gogna (1996), vertical and horizontal surface displacements are given by

$$u_x^0 = -\frac{Q_v}{L\mu}\sum_{n=1}^{N}\frac{k_n}{F_n}(4\nu_n\gamma_n e^{-\nu_n z_0} - 2(k_n^2 + \gamma_n^2)e^{-\gamma_n z_0}) \times \sin\{k_n(x - x_0)\}, \quad (19)$$

$$u_z^0 = \frac{Q_v}{L\mu}\sum_{n=1}^{N}\frac{\nu_n}{F_n}(2(k_n^2 + \gamma_n^2)e^{-\nu_n z_0} - 4k_n^2 e^{-\gamma_n z_0}) \times \cos\{k_n(x - x_0)\} - i\{Q_v k_\alpha/(\mu L k_\beta^2)\} \times \exp(-ik_\alpha z_0), \quad (20)$$

where

$$F_n = (k_n^2 + \gamma_n^2)^2 - 4k_n^2\nu_n\gamma_n. \quad (21)$$

For an internal horizontal line force $Q_H e^{i\omega t}$, applied at (x_0, z_0) in positive x-direction, the source potentials are

$$\phi_H = \frac{Q_H}{2L\mu k_\beta^2}\sum_{n=-N}^{N}(ik_n/\nu_n) \times \exp\{-\nu_n|z - z_0| - ik_n(x - x_0)\},$$

$$\psi_H = sgn(z - z_0)\frac{Q_H}{2L\mu k_\beta^2} \times \sum_{n=-N}^{N}\exp\{-\gamma_n|z - z_0| - ik_n(x - x_0)\}. \quad (22)$$

The horizontal and vertical displacements at the stress free surface are given by

$$u_x^0 = -\frac{Q_H}{L\mu}\sum_{n=1}^{N}\frac{\gamma_n}{F_n}(4k_n^2 e^{-\nu_n z_0} - 2(k_n^2 + \gamma_n^2)e^{-\gamma_n z_0}) \times\cos\{k_n(x - x_0)\} - i\{Q_H/(\mu L k_\beta)\}\exp(-ik_\beta z_0). \quad (23)$$

$$u_z^0 = -\frac{Q_H}{L\mu}\sum_{n=1}^{N}\frac{k_n}{F_n}(2(k_n^2 + \gamma_n^2)e^{-\nu_n z_0} - 4\nu_n\gamma_n e^{-\gamma_n z_0}) \times \sin\{k_n(x - x_0)\}. \quad (24)$$

Acceleration components at the surface are given by

$$A_j^0 = -\omega^2 u_j^0, \quad (j = x, z). \tag{25}$$

6. Numerical results

To observe the effects of growth of cracks leading to interconnections and their saturation on strong ground motion, I restrict numerical study to a particular model. The values for elastic moduli and density of the uncracked medium (Granite) are taken from Bullen (1963). These are

$$\lambda = 2.238 \times 10^{11}\text{dyne/cm}^2,$$
$$\mu = 2.992 \times 10^{11}\text{dyne/cm}^2,$$
$$\rho_s = 2.65\,\text{gm/cm}^3.$$

Cracks are assumed to be saturated with water. The bulk modulus and density of water are

$$\tilde{K} = 0.214 \times 10^{11}\text{dyne/cm}^2, \quad \rho_s = 1.0\,\text{gm/cm}^3.$$

Synthesis is made for 128 frequencies distributed at equal intervals for highest frequency of 10 Hertz. For each frequency, truncation number N for convergence of all infinite series {cf. equations (19), (20), (23) and (24)} is determined numerically. The source time dependence is represented by an impulse function $\delta(t)$. It is assumed that the depth of source is 2 km and the recording device is at a horizontal distance of 10 km. The distance interval $L = 50$ km between the sources provides enough time to record the disturbance from a single source at (x_0, z_0). Magnitude of particle motion depends on the value of dimensionless quantity $Q/L\mu$, whose value is assumed to be 10^{-10} both for horizontal and vertical line forces. To remove the singularities (in the summations, where $F_n = 0$), the imaginary part of the frequency is set to be -0.01 Hz. It will smoothen spectrum. Also it will enhance first motions relative to the later arrivals and hence minimize the influence of neighbouring fictitious sources. The effect of this imaginary part is removed from final time domain solution. The impulse response $g(x, z; t)$ is obtained from the complex frequency solution $G(x, z; \omega)$ through the relation

$$g(x, z; t) = e^{\omega_I t} \int_{-\infty}^{\infty} G(x, z; \omega) e^{i\omega_R t} \mathrm{d}\omega_R,$$

Integration is computed using Fast Fourier Transform.

Near-field accelerations are computed both for vertical line force and horizontal line force. Various sets of values are used to define the geometry of cracks present in the medium of propagation. These are explained as follows:

i) To study the effects of introduction and saturation of cracks accelerations are computed for three sets of parameters. These are
   (a) $\epsilon = 0$ (i.e., no cracks present);
   (b) $\epsilon = 0.2$ & $\xi = 0$ (i.e., dry cracks); and
   (c) $\epsilon = 0.2$ & $\xi = 1$ (i.e., fully saturated cracks).
   Accelerations are plotted in figures 2 and 7.

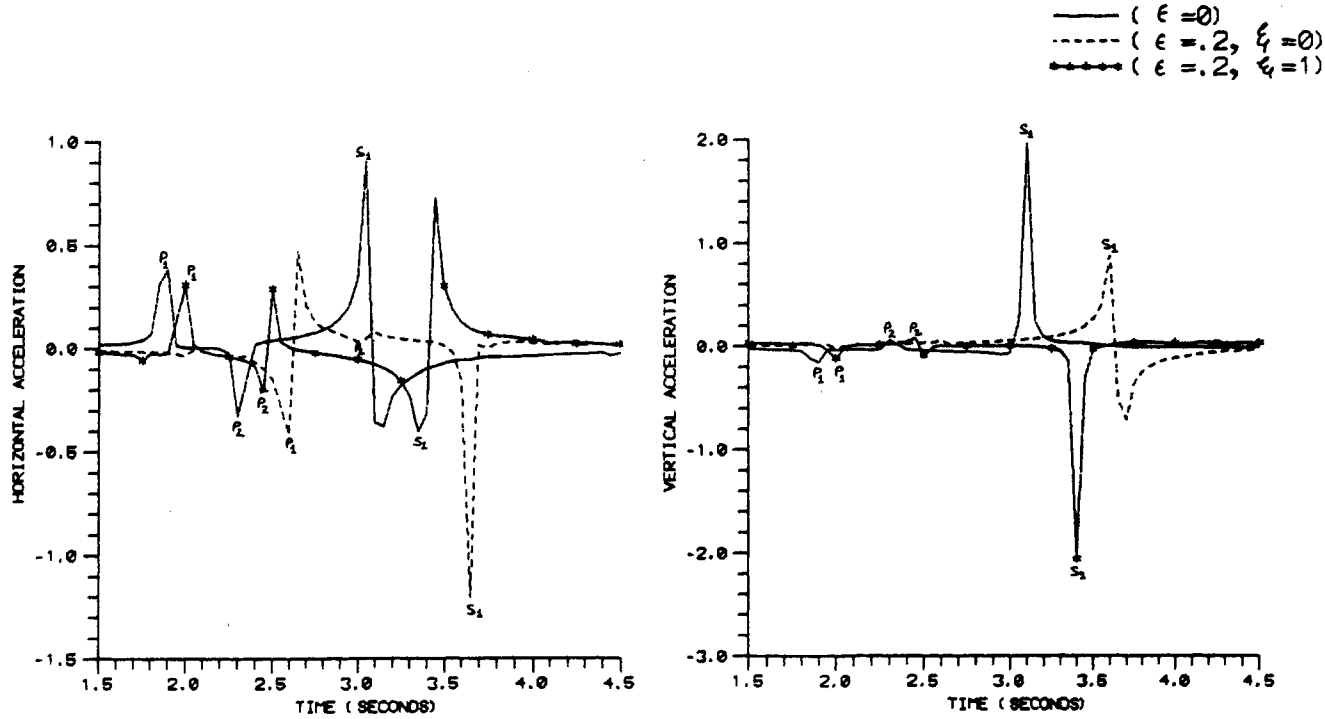

Figure 2. Effect of introduction and saturation of cracks on acceleration due to vertical line force ($c/a = 0.001$).

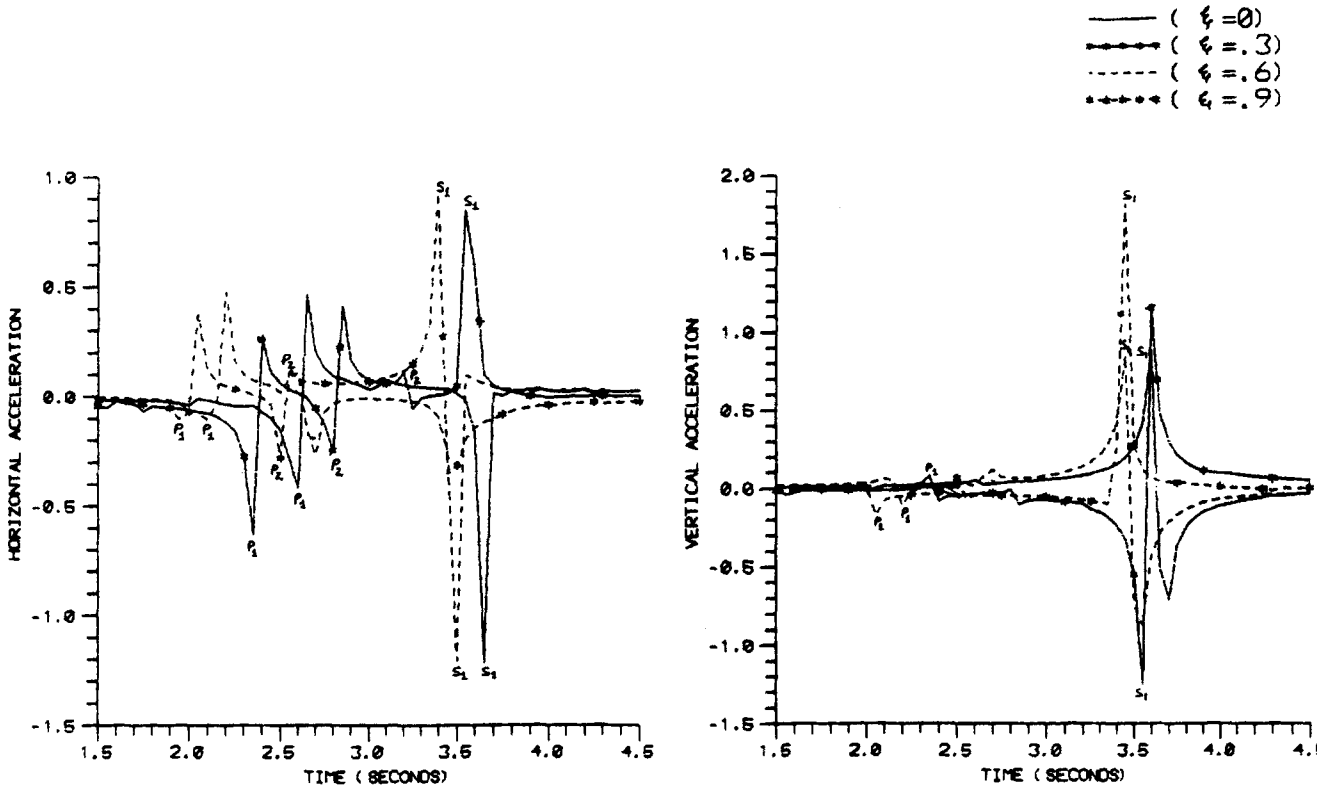

Figure 3. Effect of variations in saturation of cracks on acceleration due to vertical line force ($\epsilon = 0.2$, $c/a = 0.001$).

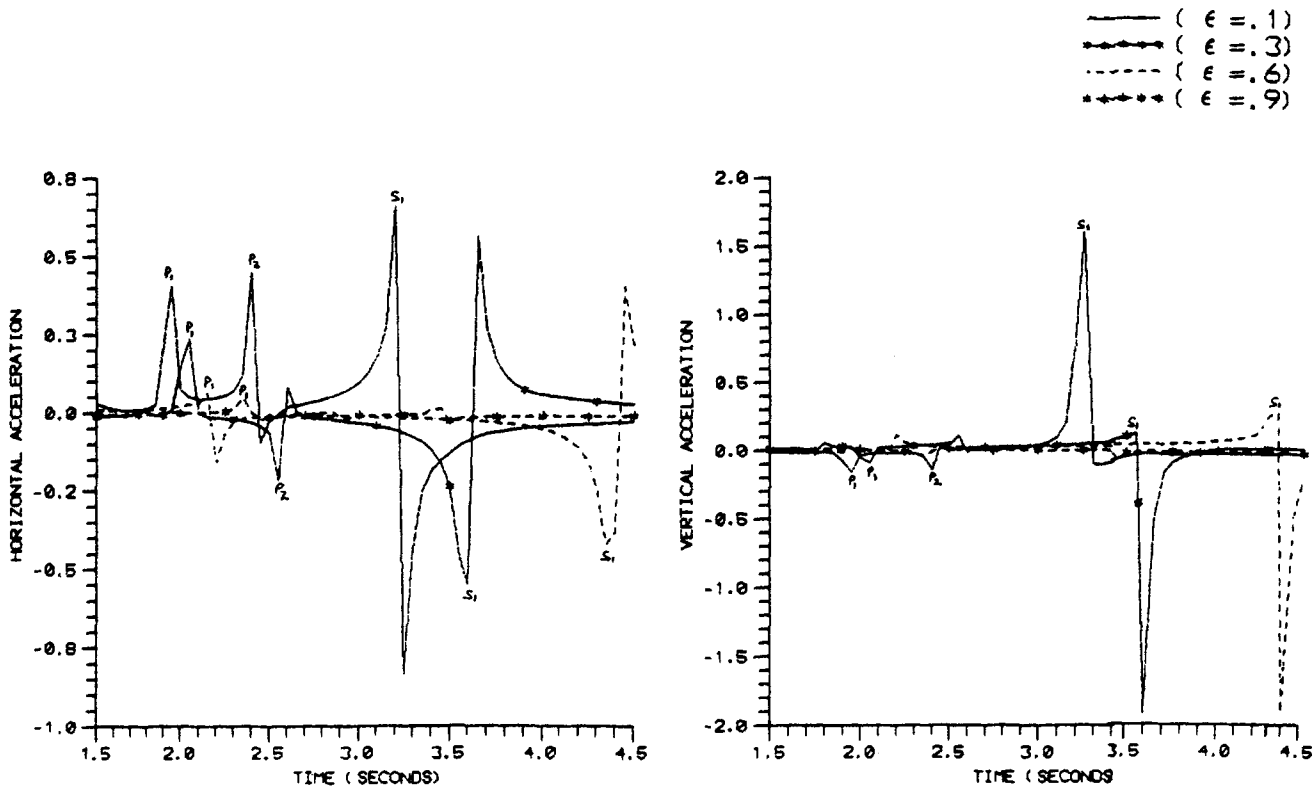

Figure 4. Effect of variations in crack density on acceleration due to vertical line force ($\xi = 1$, $c/a = 0.001$).

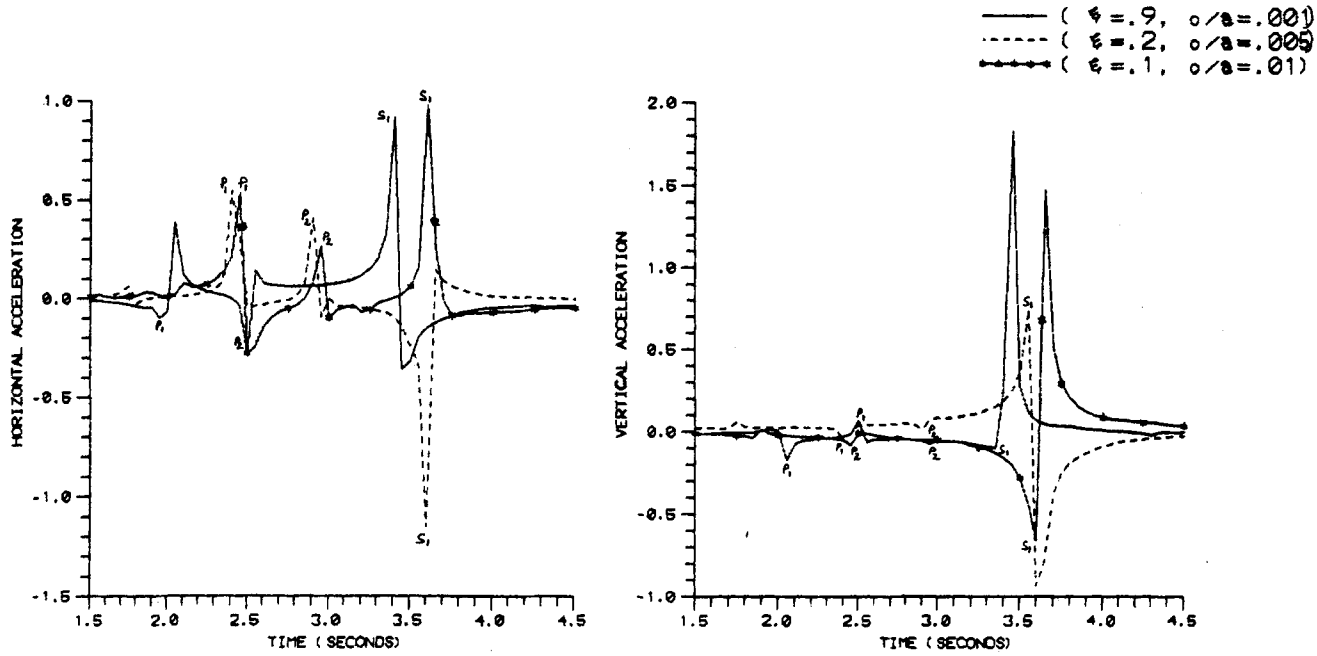

Figure 5. Effect of variations in aspect ratio of cracks on acceleration due to vertical line force ($\epsilon = 0.2$).

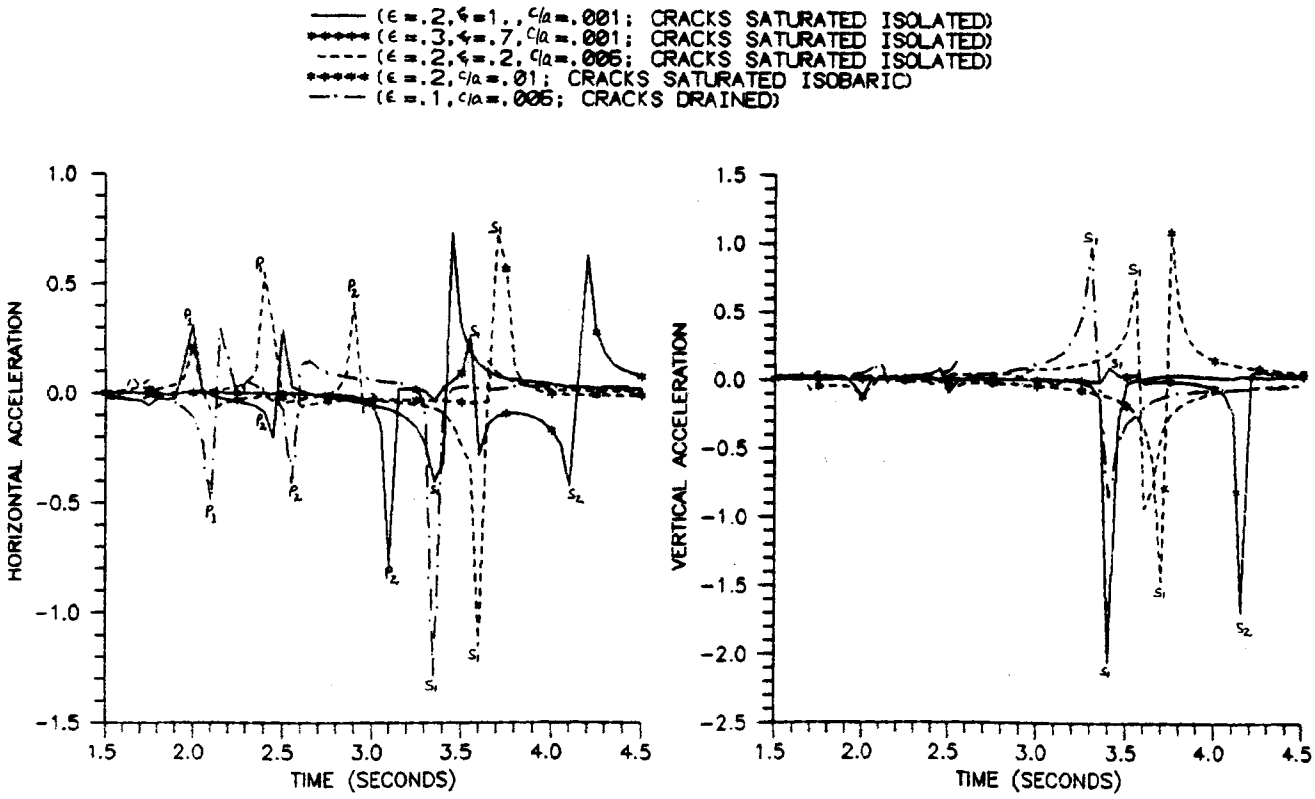

Figure 6. Variations of acceleration due to vertical line force during an earthquake preparation process.

ii) Cracks are isolated and crack density is fixed at $\epsilon = 0.2$. Aspect ratio is 0.001. Figures 3 and 8 show the variations of accelerations with different values of saturation parameter $\xi = 0$, 0.3, 0.6 and 0.9.

iii) Cracks are assumed to be nearly fully saturated (i.e., $\xi = 0.9$). Water is isolated in each crack. Aspect ratio c/a for cracks is fixed at 0.001. Different values assigned to crack density ϵ are 0.1, 0.3, 0.6 and 0.9. Variations of

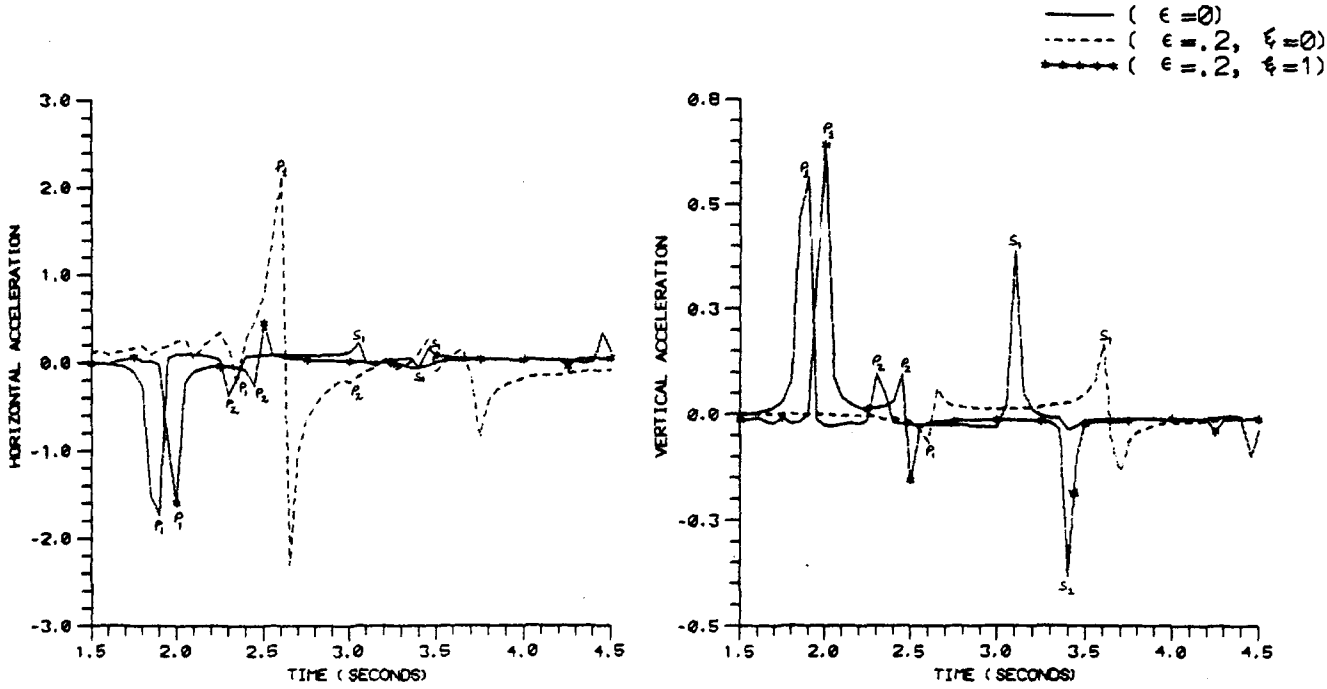

Figure 7. Effect of introduction and saturation of cracks on acceleration due to horizontal line force ($c/a = 0.001$).

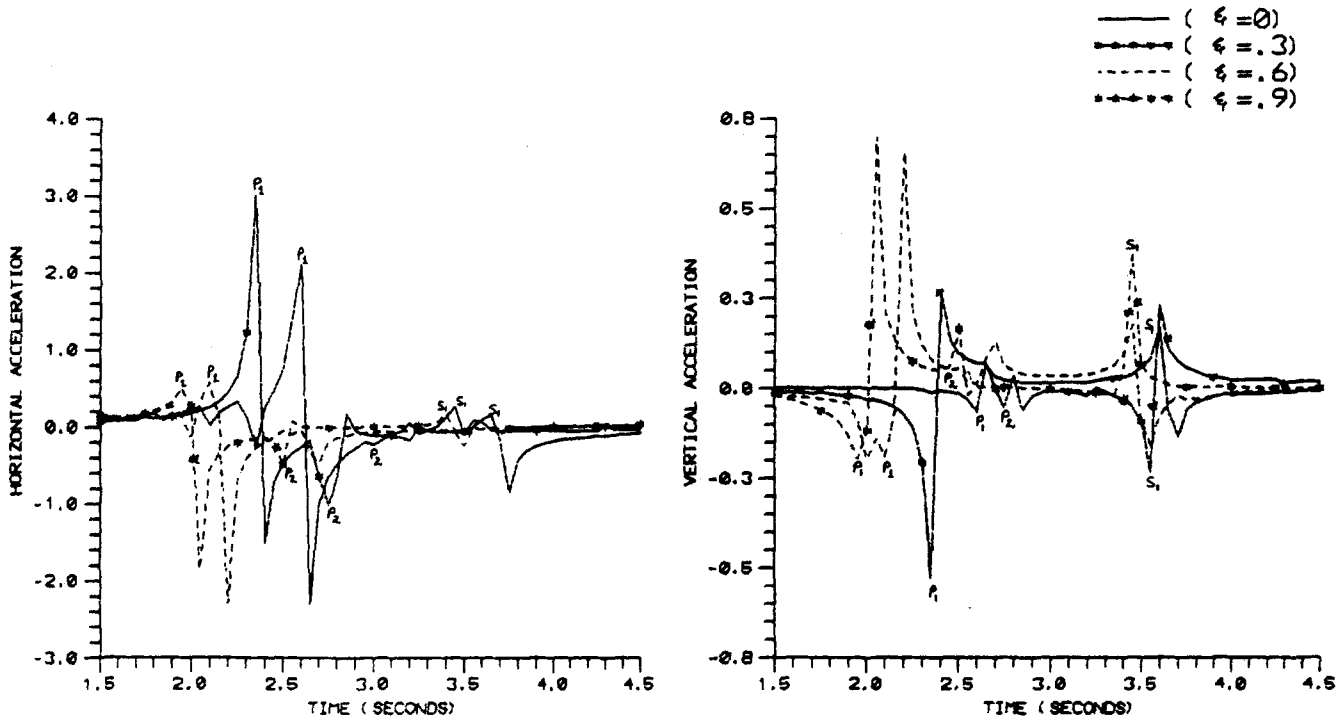

Figure 8. Effect of variations in saturation of cracks on acceleration due to horizontal line force ($\epsilon = 0.2$, $c/a = 0.001$).

accelerations with crack density are shown in figures 4 and 9.

iv) To observe the effect of crack width on ground motion, the value of crack density is fixed at 0.2. It is assumed that the change in crack width affects the saturation level. Three pairs of values of $(\xi, c/a)$ are used to compute the accelerations shown in figures 5 and 10. These values are (0.9, 0.001), (0.2, 0.005) and (0.1, 0.01).

v) This is an attempt to interpret earthquake preparation process by the change in parameters $(\epsilon, \xi$ and $c/a)$ of cracks and transition between

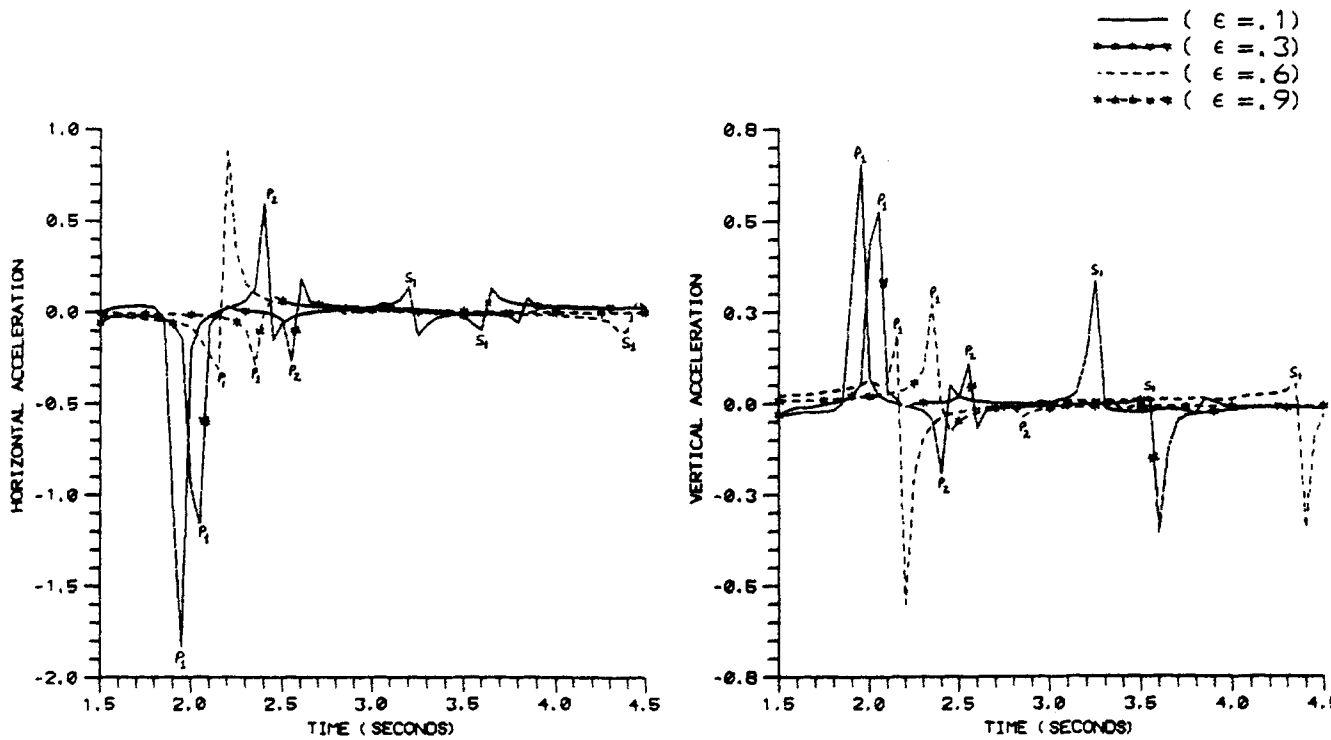

Figure 9. Effect of variations in crack density on acceleration due to horizontal line force ($\xi = 1$, $c/a = 0.001$).

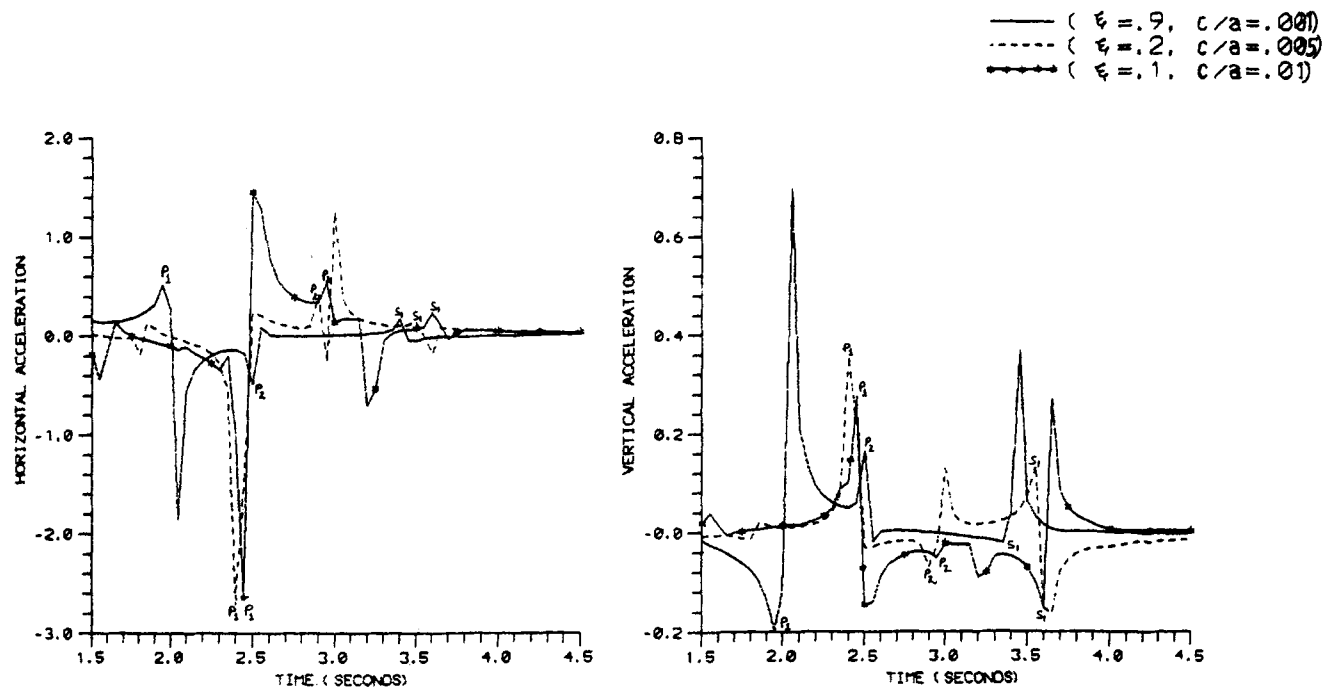

Figure 10. Effect of variations in aspect ratio of cracks on acceleration due to horizontal line force ($\epsilon = 0.2$).

different regimes of crack interconnections. The whole process is assumed to be passing through five major stages. Stage I represents an ordinary cracked medium with $\epsilon = 0.2$, $\xi = 1$ and $c/a = 0.001$. Ratio of the velocity of compressional wave to the velocity of shear wave is nearly 1.75 in this stage. It may be noted that for the assumed values of elastic parameters this velocity ratio for an elastic medium in the absence of cracks is found to be 1.66 approximately.

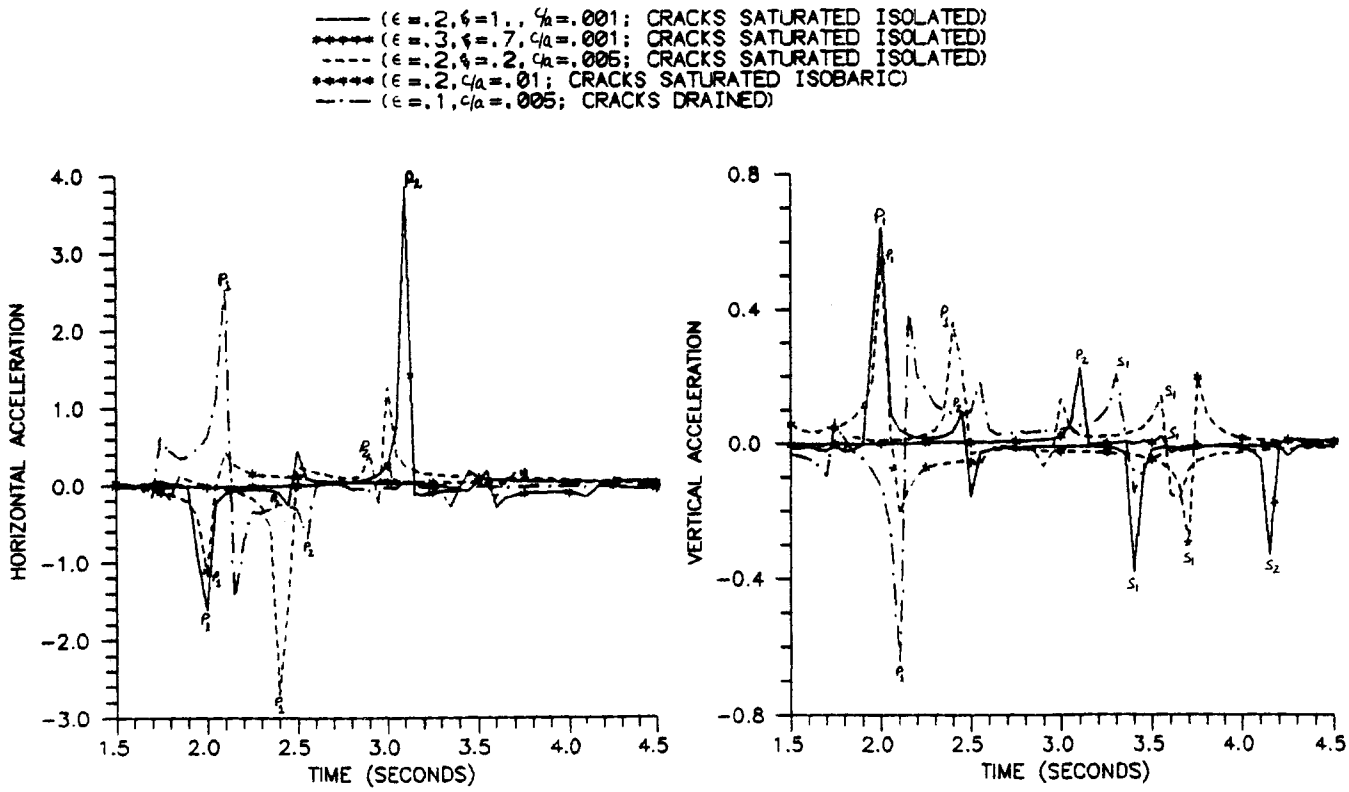

Figure 11. Variations of acceleration due to horizontal line force during an earthquake preparation process.

Accumulation of stress results in crack growth and hence undersaturation. This is stage II and is fixed by $\epsilon = 0.3$, $\xi = 0.7$ and $c/a = 0.001$. Velocity ratio in this stage is found to be 1.64. Further increase of stress results in the enhancing of width of cracks and again reduces saturation level. It is assumed that crack density may be reduced by the healing of undersaturated cracks. This stage III having the velocity ratio nearly 1.49 is represented by $\epsilon = 0.2$, $\xi = 0.2$ and $c/a = 0.005$. Before an earthquake, stresses are assumed enough to develop connections between cracks. This is stage IV and regime for connections of cracks is saturated isobaric with flow of liquid allowed between cracks to lubricate the fault surface for eventual failure. Parameters' values are assumed to be $\epsilon = 0.2$, and $c/a = 0.01$. Velocity ratio in stage IV is found to be approximately 1.84. The last stage considers the crack geometry just after the main shock. The cracks are assumed in drained regime with liquid drained out of cracks to fill the fault. This stage V, represented by $\epsilon = 0.1$ and $c/a = 0.005$, assumes the healing and closure of drained cracks. The velocity ratio decreases to 1.6 approximately. It is likely that an earthquake may take place between stage IV and stage V. Around stage V increase in velocity ratio can be expected which indicates that after the earthquake the drained cracks may be healed to become saturated and isolated again. Accelerations for all the five stages are shown in figures 6 and 11.

7. Discussion of numerical results

In all the accelerograms four signals can be noticed. First and third signals (P_1 and S_1) are arrival of P and S waves respectively, reaching recording station diagonally from source. Second and fourth signals (P_2 and S_2) are also P and S waves respectively but these waves first travel vertically above from the source to free surface and then along the surface to station. Signal S_2 is significant in few cases.

Variations in accelerations for different combinations of crack density (ϵ), saturation parameter (ξ), aspect ratio (c/a) and for an assumed earthquake preparation process are discussed as follows:

- When source is a vertical line force, variations in horizontal and vertical accelerations are as follows:

Contribution of P waves to vertical acceleration is negligible and hence only S waves significantly contribute to vertical acceleration. Introduction of dry cracks delays the arrival of both P and S waves. This delay is reduced when cracks are saturated. Presence of dry cracks increases the horizontal acceleration but decreases the vertical acceleration due to S waves. Acceleration in the presence of fully saturated cracks ($\epsilon = 0.2$) is almost similar to

that observed in the absence of cracks. Increase in saturation level decreases the times of travel of both P and S waves. Magnitude of horizontal acceleration is not much affected with the increase of ξ.

Increase of ϵ increases the time of travel of both P and S waves. Horizontal acceleration decreases with the increase of ϵ but vertical acceleration changes only direction. This change in the direction of particle motion indicates the anisotropic behaviour of wave propagation in a cracked solid. Widening of cracks is coupled with reduction in saturation level. It delays the signal of both P and S waves. Horizontal acceleration is almost unaffected with the change in the width of cracks. Vertical acceleration due to S waves decreases with the increase in the width of cracks.

During the assumed earthquake process we note that the velocity ratio of P wave to that of S wave decreases for the first three stages and reaches the lowest value of 1.49. It then recovers to get the highest value in stage IV and starts decreasing just before the earthquake. The magnitude of horizontal acceleration, due to P wave, decreases rapidly for stage II and then recovers for stages III to V. The second arrival of P waves shows maximum horizontal acceleration in stage II. Horizontal acceleration due to S wave increases for stages I to III and then decreases slightly for stage IV to recover again. Stage II can also be identified with vertical acceleration which assumes minimum value for first arrival and maximum value for second arrival of S waves.

- When source is a horizontal line force, the variations in horizontal and vertical accelerations are as follows:

S wave contribution to horizontal acceleration is negligible. Presence of fluid-filled cracks ($\epsilon = 0.2$) does not have much effect on acceleration but the effect is large when cracks are dry. Introduction of dry cracks increases the horizontal acceleration due to first arrival of P waves only. At the same time vertical acceleration is minimum when cracks are dry. Increase in ξ decreases the time of travel of both P and S waves and increases the vertical acceleration as well. The horizontal acceleration increases with ξ up to a certain level but the increase of ξ beyond this level slowly reduces the acceleration.

Increase in ϵ decreases the magnitude of horizontal acceleration. Vertical acceleration decreases with the increase of ϵ up to a reasonable level. S wave arrivals suffer much longer delays as ϵ increases. The magnitude of horizontal acceleration increases with the widening of cracks. With the increase in width of cracks vertical acceleration due to S waves decreases. However, a stage may come when more widening of cracks shows no effects on accelerations. Vertical acceleration due to P waves decreases with the widening of cracks.

During an assumed earthquake preparation process, stage II is represented by minimum acceleration in the first arrival and maximum acceleration in the second arrival. The vertical acceleration due to P waves after decreasing rapidly for stage II starts increasing with the stages from III to V. Only the first arrival of P waves significantly contributes to horizontal acceleration except in stage II. Contribution of S waves to vertical acceleration decreases with the advancement of stages.

8. Conclusions

From the above discussion of variations exhibited in figures 2 to 11, the following conclusions may be drawn:

- Contribution of P waves to vertical acceleration is negligible when the source is vertical line force.
- When source is horizontal line force contribution of S waves to horizontal acceleration is negligible.
- Presence of dry cracks affects acceleration to a large extent. Saturation up to a certain level affects the acceleration but for higher saturation level these effects may disappear.
- Increase of saturation speed up the travel of both P and S waves.
- Increase of crack density of fully saturated cracks decreases the velocity of S waves to a greater extent. It also decreases horizontal acceleration but does not affect the magnitude of vertical acceleration due to S waves.
- Widening of cracks up to a certain width increases the horizontal acceleration and decreases the vertical acceleration. More increase in width may have no effect or opposite effects.
- Travel time or velocity ratio anomalies observed during the assumed five stages verify the assumed stages of earthquake preparation process. Stage II can be easily distinguished and hence may suggest the initial stage of earthquake preparation. Magnitude of P and S wave signals in vertical and horizontal direction may indicate the nature of the forces operating at the focus and the different stages of the earthquake preparation as well.

In this study a more realistic model of a focal region is considered. Accelerograms are studied for general sources because results for realistic sources can be constructed from these general sources. An assumed earthquake process is verified through travel time anomalies and stages of earthquake preparation process are identified with variations in near-field ground motion. This will help to simulate the actual process of stress accumulation leading to eventual failure. This piece of work may be useful in the studies leading to prediction of earthquakes.

Acknowledgements

This work is financially supported by the Department of Science and Technology, Govt. of India, under the project HR/OY/A-01/95.

References

Aggarwal Y P, Sykes L R, Armbruster J and Sbar M L 1973 Premonitory changes in seismic velocities and prediction of earthquakes; *Nature (London)* **241** 101–104

Bouchon M and Aki K 1977 Discrete wave-number representation of seismic-source wave fields; *Bull. Seism. Soc. Am.* **67** 259–277

Budiansky B and O'Connell R J 1976 Elastic moduli of dry and saturated cracked solids; *Int. J. Solids Struct.* **12** 81–97

Bullen K E 1963 An Introduction to Theoretical Seismology. C.U.P.

Burridge R and Knopoff K 1964 Body force equivalents for seismic dislocations; *Bull. Seism. Soc. Am.* **54** 1875–1888

Chatterjee A K, Knopoff M L and Hudson J A 1980 Attenuation of elastic waves in a cracked, fluid-saturated solid; *Math. Proc. Camb. Philos. Soc.* **88** 547–561

Crampin S 1985 Evidence for aligned cracks in Earth's crust; *First Break* **3** 12–15

Crampin S 1987 The basis for earthquake prediction; *Geophys. J. R. Astron. Soc.* **91** 331–347

Crampin S and Atkinson B K 1985 Microcracks in the Earth's crust; *First Break* **3** 16–20

Garvin H D and Knopoff L 1973 The compressional modulus of a material permeated by a random distribution of circular cracks; *Q. Appl. Math.* **30** 453–464

Garvin H D and Knopoff L 1975a The shear modulus of a material permeated by a random distribution of free circular cracks; *Q. Appl. Math.* **33** 296–300

Garvin H D and Knopoff L 1975b Elastic moduli of a medium with liquid filled cracks; *Q. Appl. Math.* **33** 301–303

Hudson J A 1981 Wave speed and attenuation of elastic waves in material containing cracks; *Geophys. J. R. Astron. Soc.* **64** 133–150

Hudson J A 1990a Overall elastic properties of isotropic materials with arbitrary distribution of circular cracks; *Geophys. J. Int.* **102** 465–469

Hudson J A 1990b Attenuation due to second order scattering in materials containing cracks; *Geophys. J. Int.* **102** 485–490

Nur A 1972 Dilatancy, pore fluids and premonitory variations of t_s/t_p travel times; *Bull. Seism. Soc. Am.* **62** 1217–1222

O'Connell R J and Budiansky B 1974 Seismic velocities in dry and saturated cracked solids; *J. Geophys. Res.* **79** 5412–5426

O'Connell R J and Budiansky B 1977 Viscoelastic properties of fluid saturated cracked solids; *J. Geophys. Res.* **82** 5719–5735

Peacock S and Hudson J A 1990 Seismic properties of rocks with distribution of small cracks; *Geophys. J. Int.* **102** 471–485

Sharma M D 1996 Surface wave propagation in a cracked poroelastic half-space lying under a uniform layer of fluid; *Geophys. J. Int.* **127** 31–39

Sharma M D and Gogna M L 1996 Discrete wave number representation of seismic source wave-fields in a fluid saturated porous media; *Indian J. Pure Appl. Math.* **27** 913–929

Xu S and King M S 1990 Attenuation of elastic waves in a cracked solid; *Geophys. J. Int.* **101** 169–180

MS received 25 July 1996; revised 13 January 1997